



University of  
**Salford**  
MANCHESTER

# Island rule and bone metabolism in fossil murines from Timor

Miskiewicz, JJ, Louys, J, Beck, RMD, Mahoney, P, Aplin, K and O'Connor, S

<http://dx.doi.org/10.1093/biolinnean/blz197>

<b>Title</b>	Island rule and bone metabolism in fossil murines from Timor
<b>Authors</b>	Miskiewicz, JJ, Louys, J, Beck, RMD, Mahoney, P, Aplin, K and O'Connor, S
<b>Type</b>	Article
<b>URL</b>	This version is available at: <a href="http://usir.salford.ac.uk/id/eprint/56252/">http://usir.salford.ac.uk/id/eprint/56252/</a>
<b>Published Date</b>	2020

USIR is a digital collection of the research output of the University of Salford. Where copyright permits, full text material held in the repository is made freely available online and can be read, downloaded and copied for non-commercial private study or research purposes. Please check the manuscript for any further copyright restrictions.

For more information, including our policy and submission procedure, please contact the Repository Team at: [usir@salford.ac.uk](mailto:usir@salford.ac.uk).

**Island rule and bone metabolism in fossil murines from Timor**

Justyna J. Miskiewicz<sup>1\*</sup>, Julien Louys<sup>2</sup>, Robin M. D. Beck<sup>3</sup>, Patrick Mahoney<sup>4</sup>, Ken Aplin<sup>\*\*</sup>, Sue O'Connor<sup>5,6</sup>

<sup>1</sup>School of Archaeology and Anthropology, College of Arts and Social Sciences, Australian National University, 0200 Canberra, Australian Capital Territory, Australia

<sup>2</sup>Australian Research Centre for Human Evolution, Environmental Futures Research Institute, Griffith University, 4111 Brisbane, Queensland, Australia

<sup>3</sup>School of Environment and Life Sciences, University of Salford, Salford M5 4WX, United Kingdom

<sup>4</sup>School of Anthropology and Conservation, University of Kent, Canterbury CT2 7NR, United Kingdom

<sup>5</sup>Archaeology and Natural History, College of Asia and the Pacific, Australian National University, 0200 Canberra, Australian Capital Territory, Australia

<sup>6</sup>ARC Centre of Excellence for Australian Biodiversity and Heritage, Australian National University, 0200 Canberra, Australian Capital Territory, Australia

\*Corresponding author. E-mail: [Justyna.Miskiewicz@anu.edu.au](mailto:Justyna.Miskiewicz@anu.edu.au)

\*\*Deceased

Running title: **Island rule and fossil murine bone metabolism**

**ABSTRACT**

Skeletal growth rates reconstructed from bone histology in extinct insular hippopotamids, elephants, bovids, and sauropods have been used to infer dwarfism as a response to island conditions. Limited published records of osteocyte lacunae densities (Ot.Dn), a proxy for living osteocyte proliferation, have suggested a slower rate of bone metabolism in giant mammals. Here, we test whether insularity may have affected bone metabolism in a series of small to giant murine rodents from Timor. Ten adult femora were selected from a fossil assemblage dated to the Late Quaternary (ca. 5–18 ka). Femur morphometric data were used in computing phylogenetically-informed body mass regressions, although phylogenetic signal was very low (Pagel's lambda = 0.03). Weight estimates calculated from these femora ranged from 75g to 1188g. Osteocyte lacunae densities from midshaft femur histological sections were evaluated against bone size and estimated body weight. Statistically significant ( $p < 0.05$ ) and strongly negative relationships between Ot.Dn, femur size, and estimated weight were found. Larger specimens were characterised by lower Ot.Dn, indicating that giant murines from Timor may have had a relatively slow pace of bone metabolic activity, consistent with predictions made by the island rule.

**Keywords:** bone histology, gigantism, insularity, Murinae, osteocyte lacunae, Late Pleistocene, Late Quaternary

## INTRODUCTION

Island ecology and biogeography have long served as models for investigating species richness, extinction, speciation, conservation and evolutionary biology (Brown & Kodric-Brown, 1977; Whittaker & Fernández-Palacios, 2007; Sax & Gaines, 2008; MacArthur & Wilson, 2016). Islands are ideal examples of isolated ecosystems that can trigger similar behavioural and biological responses across different animals (Whittaker & Fernández-Palacios, 2007; Miller & Spoolman, 2011; MacArthur & Wilson, 2016). Foster (1964) was the first to discuss body size shifts in species affected by insularity. Van Valen (1973) formalised this under the island rule, which is now known as one of the most fundamental theories in evolutionary biology (Clegg & Owens, 2002; Schillaci *et al.* 2009; Benton *et al.* 2010). It posits that large and small insular mammals decrease and increase their body size, respectively, to accommodate resource availability and drive optimal life histories. Sondaar (1977) then provided a broader perspective on mammal insularity and diversification, highlighting the need to consider islands based on their “oceanic and continental” (p. 617) origin, but study each one within its own context due to complex island histories. Lomolino’s (1985, Lomolino *et al.* 2013) later re-examination and re-definition of the island rule specifically encompassed a dwarfism – gigantism gradient (see Lokatis & Jeschke, 2018 for review). Some issues relating to biological constraints limiting a species’ plasticity (Meiri *et al.* 2004; 2008), otherwise known as phylogenetic inertia (Darwin, 1859), have since also been considered.

Inferring the cause of body size change in relation to insularity has been subject to much discussion (e.g. Lomolino, 1985; 2013; Millien & Damuth, 2004; Meiri *et al.* 2004; 2006; Itescu *et al.* 2014; Faurby & Svenning, 2016). Trends in body size changes on islands are often

Miszkievicz et al BJLS R2 Page 3 of 37

1  
2  
3 46 associated with data scatter, likely representing multiple factors contributing to an animal's  
4  
5 47 body mass. These include inter-island differences in competition for resources and mating  
6  
7 48 opportunities, resource availability, geographical factors such as island size and distance from  
8  
9 49 other islands or the mainland, latitude, and climate (McNab, 1971; 2010). In cases of adaptive  
10  
11 50 radiation from a single ancestor, it is also possible for organisms to rapidly diversify into both  
12  
13 51 giant and small forms. Only in conditions of ecological release and time in isolation could body  
14  
15 52 mass trend lines be fitted perfectly (Lomolino, 2005).  
16  
17  
18  
19  
20

21 53  
22 54 When applying the island rule to birds and mammals, which have high resource requirements  
23  
24 55 associated with high metabolic rates compared to other terrestrial vertebrates, body mass is a  
25  
26 56 good indicator of life history and energetic investment (McNab, 2019). Body mass closely  
27  
28 57 reflects basal metabolic rate (BMR) in endotherms, which generate and regulate heat internally  
29  
30 58 to satisfy energetic demands that are required for survival and reproduction (McNab, 2019).  
31  
32 59 Body mass measures, including estimates from fossil material, and large scale meta-analyses  
33  
34 60 have demonstrated gigantism and dwarfism in multiple species globally (Yabe, 1994; Boback  
35  
36 61 & Guyer, 2003; Lomolino 2005; Palombo, 2007; Köhler & Moyà-Solà, 2009; van der Geer *et*  
37  
38 62 *al.*, 2013). Histology techniques in particular have also proven valuable in reconstructing  
39  
40 63 metabolic activity of the once living bone tissues of different species and taxa by capturing cell  
41  
42 64 metabolic activity indicators preserved in their fossils (e.g. Köhler & Moyà-Solà, 2009; Benton  
43  
44 65 *et al.* 2010; Orlandi-Oliveras *et al.* 2016).  
45  
46  
47  
48  
49  
50

### 51 67 **The island rule and rodents**

52  
53 68 Island rodents, particularly mice, rats, and related species (superfamily Muroidea) have been  
54  
55 69 of particular interest for addressing physiological, morphological, and behavioural responses

1  
2  
3 70 to island ecology (Adler & Levins, 1994; Renaud & Millien, 2001; Abdelkrim *et al.* 2005;  
4  
5 71 Harper *et al.* 2005; Towns *et al.*, 2006; Firmat *et al.* 2010; Moncunill-Solé *et al.* 2014; Swift *et*  
6  
7  
8 72 *al.* 2018; van der Geer, 2018; Geffen & Yom-Tov, 2019). Because of their relatively short  
9  
10 73 lifespans, high level of reproduction, and multiple adaptive radiations, they are important  
11  
12 74 models for studying animal environmental plasticity (Mizkiewicz *et al.* 2019; van der Geer  
13  
14 75 2019). Comparisons between insular and mainland rodent populations have focused on  
15  
16 76 reproductive behaviour (Stamps & Buechner, 1985) and morphology (Lomolino, 1984),  
17  
18 77 collectively termed the “island syndrome” (Adler & Levins, 1994; Adler, 1996; Russell *et al.*  
19  
20 78 2011). Isolated insular rodent populations experience a demographic increase in density and  
21  
22 79 dispersal, improved survival and associated reproduction rates, minimised inter-specific  
23  
24 80 competition, and an increase in body mass the more isolated and smaller the island (Foster,  
25  
26 81 1964). However, there have also been cases of insular rodents that evolved into dwarfed forms  
27  
28 82 (e.g. *Perognathus* spp. on islands bordering Mexico) due to food supply limitations in  
29  
30 83 heterogeneous environments (Lawlor, 1982; Durst & Roth, 2015). Adaptive shifts in rodent  
31  
32 84 morphology and/or behaviour are short or long term depending on the time scale, sample, and  
33  
34 85 context investigated (Palkovacs, 2003). Rodent size adaptation probably occurs initially as a  
35  
36 86 short-term phenotypic change in response to increased island population density. Longer time  
37  
38 87 scale natural selection favouring increased body size would follow when mortality rates and  
39  
40 88 predation are stable and low, as they are on islands (Brown & Sibly, 2006).

41  
42  
43  
44  
45  
46  
47 89  
48  
49 90 Foster’s (1964) report of insular mammal gigantism was based on observations of two species  
50  
51 91 of deer mice (*Peromyscus maniculatus* and *P. sitkensis*) of the Queen Charlotte Islands in  
52  
53 92 Canada. Almost double the size of *P. maniculatus*, *P. sitkensis* was found on the outer small  
54  
55 93 and dispersed islands. Foster (1964) suggested a depauperate fauna, reduced competition for

1  
2  
3 94 resources, and minimised predation on small islands favoured insular gigantism as a selective  
4  
5 95 advantage. Empirical evidence for rodent body mass change has since been reported for several  
6  
7 96 other species spanning many geographical locations (e.g. Ventura & Fuster, 2000; Michaux *et*  
8  
9 97 *al.* 2002; Millien & Damuth, 2004; Russell *et al.* 2011; Pergams *et al.* 2015). Body size increase  
10  
11 98 on small islands has been observed in Japanese *Apodemus speciosus* (Millien & Damuth,  
12  
13 99 2004), black rats (*Rattus rattus*) in the Mozambique Channel (Russell *et al.* 2011), Polynesian  
14  
15 100 rat *R. exulans* and black rat *R. rattus* in New Zealand and the Pacific islands (Yom-Tov *et al.*  
16  
17 101 1999), Californian *R. rattus* from Anacapa Island (Pergams *et al.* 2015), woodmouse  
18  
19 102 (*Apodemus sylvaticus*) in the Western Mediterranean Sea (Michaux *et al.* 2002), and *R. rattus*  
20  
21 103 from Congreso Island in Spain (Ventura & Foster, 2000). Skeletal biology literature of island  
22  
23 104 fossil rats mostly reports gross anatomy and morphometric data used for taxonomic purposes.  
24  
25 105 Measurements of dental material (Millien & Damuth, 2004; Louys *et al.* 2018), and cranial and  
26  
27 106 post-cranial morphology (Bocherens *et al.* 2006; Aplin & Helgen, 2010) have been used in  
28  
29 107 taxonomic assignments, but these data have proven equally informative about locomotion, diet,  
30  
31 108 and ecology of rodents such as the case of a now well-studied extinct giant genus *Mikrotia*  
32  
33 109 from the Gargano peninsula (Zafonte and Masini, 1992; Parra *et al.* 1999; Moncunill-Solé *et*  
34  
35 110 *al.* 2018). Very large, insular members of the murid subfamily Murinae have been reported  
36  
37 111 from the fossil record at multiple locations throughout the world, including the Flores giant rat  
38  
39 112 (*Papagomys armandvillei*) in Indonesia (Locatelli *et al.* 2012), *Coryphomys* from Timor (Aplin  
40  
41 & Helgen, 2010), the Tenerife giant rat (*Canariomys bravoii*) from the Canary Islands  
42  
43 113 (Bocherens *et al.* 2006; Firmat *et al.*, 2011). *Megalomys* is a member of another muroid family,  
44  
45 114 Cricetidae, and is known from five very large species from the West Indies (van den Hoek  
46  
47 115 Ostende *et al.* 2017). Some extant giant muroid species that had colonised their islands in the  
48  
49 116 Late Pleistocene or earlier include *Diplothrix legata*, *Apodemus speciosus* and *Apodemus*  
50  
51  
52  
53  
54  
55  
56  
57  
58  
59  
60

1  
2  
3 118 *argenteus* in Japan (Kawamura, 1991), *Phloeomys cumingi* and *P. pallidus* in the Philippines  
4  
5 119 (Rickart & Heaney, 2002), and *Hypogeomys antimena* in Madagascar (Sommer *et al.* 2002).  
6  
7  
8 120

9  
10 121 **Bone histology and insular fossil animals**  
11

12 122 Histological sectioning of fossil bone has proven successful for the reconstruction of tetrapod  
13  
14 123 palaeobiology (Chinsamy-Turan, 2011; de Ricqlès, 2011). By studying microscopic structures  
15  
16 124 and composition in bone samples of fossil vertebrates, skeletal maturation, seasonality,  
17  
18 125 behaviour, and bone metabolism can be reconstructed (Chinsamy-Turan, 2011; Köhler *et al.*  
19  
20 126 2012). As bone tissue forms, matures, and remodels throughout an animal's lifespan, this  
21  
22 127 information is reflected in the density, organisation, morphology, and geometric properties of  
23  
24 128 bone microstructure (Enlow & Brown, 1956; 1957; 1958). This approach has been successfully  
25  
26 129 applied in insularity contexts (see Kolb *et al.* 2015 for review). For example, slow bone growth  
27  
28 130 rates indicate delayed maturity and extended lifespans in the Late Pleistocene dwarfed Balearic  
29  
30 131 island "goat" (*Myotragus balearicus*) (Köhler, 2010; Köhler & Moyà-Solà, 2009), and insular  
31  
32 132 dwarfism in the Late Jurassic sauropod *Europasaurus holgeri* (Sander *et al.* 2006). To the best  
33  
34 133 of our knowledge, quantitative palaeohistological analyses in relation to island ecology have  
35  
36 134 not been performed for island fossil rodents. Prior research in extinct giant rodent cases  
37  
38 135 reported bone tissue only in the Late Miocene murine *Mikrotia magna* from Gargano Island in  
39  
40 136 Italy (Kolb *et al.*, 2015). We also recently (Miszkievicz *et al.* 2019) reported descriptions of  
41  
42 137 bone remodeling in one of the giant murines (ANU TDS 0-30 #4) in comparison to a small  
43  
44 138 murine femur (ANU TDD 1 #11) from the same assemblage analysed in the present research.  
45  
46 139 Orlandi-Oliveras *et al.* (2016) observed bone histology of the fossil giant dormouse *Hypnomys*  
47  
48 140 *onicensis* (Gliridae) from the Balearic Islands indicating increased lifespan that may have been  
49  
50 141 a result of gigantism. While these previous studies have included the description of bone tissue  
51  
52  
53  
54  
55  
56  
57  
58  
59  
60

Miszkievicz *et al.* BJLS R2 Page 7 of 37



1  
2  
3 142 types and their organisation, the quantification of osteocyte lacunae within the bone matrix in  
4  
5 143 relation to insularity remains to be tested.  
6  
7

8 144

9  
10 145 Prior research exploring osteocyte lacunae densities (Ot.Dn) has revealed relationships  
11  
12 146 between this measure of bone metabolic activity and negative relationships with body in non-  
13  
14 147 insular settings that may be ultimately linked to aspects of life history. Inter-specific studies of  
15  
16 148 fast maturing and small-bodied, and slow maturing and large-bodied mammal species, exhibit  
17  
18 149 higher and lower osteocyte densities, respectively (Mullender *et al.* 1996; Bromage *et al.* 2009).  
19

20  
21 150 This phenomenon may reflect an underlying complex relationship between bone ontogeny,  
22  
23 151 rates of metabolism and cell proliferation that are related to body mass (Bromage *et al.* 2009).  
24

25  
26 152 For example, Ot.Dn decreased with increased body size when compared across selected non-  
27  
28 153 primate mammalian species (Mullender *et al.* 1996). Bromage *et al.* (2009: 393) reported an  
29

30  
31 154 average of 58,148/mm<sup>3</sup> osteocytes in three females of *R. norvegicus* that had an average body  
32  
33 155 weight of 300 g. In contrast, a hippo (*Hippopotamus amphibius*) with a body weight of 2000  
34

35  
36 156 kg, exhibited 16,667/mm<sup>3</sup> osteocytes (Bromage *et al.*, 2009: 393). Furthermore, experimental  
37  
38 157 findings suggest a relationship whereby bone and energy homeostasis is regulated through  
39

40  
41 158 hormones that are involved both in bone cell biology and body mass accrual (Hogg *et al.*, 2017;  
42  
43 159 see their Figure 11.1). Taken together, these studies suggest a strong inter-specific relationship  
44

45 160 between Ot.Dn and body size in mammals. This relationship offers therefore a unique way to  
46  
47 161 investigate the growth of fossil rats from island settings.  
48

49 162

### 51 163 **Hypothesis and prediction**

52  
53 164 The goal of this study was to evaluate the island rule using Timorese fossil murine rodents  
54  
55 165 whose body size would have ranged from small to giant, as inferred from their bone size. We  
56  
57

1  
2  
3 166 studied osteocyte lacunae preserved in femoral midshaft samples to determine if bone  
4  
5 167 metabolic activity, indicative of tissue growth and related to life history, is related with body  
6  
7  
8 168 size among insular members of the rodent subfamily Murinae. We predicted that larger bodied  
9  
10 169 fossil specimens would have a slower rate of osteocyte proliferation compared to those with a  
11  
12 170 smaller body.

13  
14  
15 171

## 16 17 172 **MATERIALS AND METHODS**

### 18 19 173 **Samples**

20  
21 174 We examined specimens that represent multiple species in the rodent subfamily Murinae from  
22  
23 175 naturally accumulated late Quaternary fossil deposits of Matja Kuru TD on Timor Island.  
24  
25  
26 176 Timor Island is located in eastern Wallacea, a region compromised of over 17,000 islands.  
27  
28 177 Having never been connected to Southeast Asia (SEA) or Australia, these islands represent  
29  
30 178 permanently isolated geographical regions. Fossil material from this assemblage date to a  
31  
32 179 minimum of ca. 5–18 ka (Louys *et al.* 2017). It was impossible to positively identify the murine  
33  
34 180 species from postcranial elements, so we could not assign them to species or genus. Murine  
35  
36 181 fossil material from Timor includes representatives of four giant extinct genera, of which only  
37  
38 182 *Coryphomys* has been formally described with two species currently recognised, *C. buehleri*  
39  
40 183 and *C. musseri* (Schaub 1937; Aplin and Helgen 2010). We have no way of estimating the  
41  
42 184 potential sex of our specimens, so we cannot exclude sexual dimorphism as a confounding  
43  
44 185 factor in our analyses. However, we note that previous research indicates it to be insignificant  
45  
46 186 in small mammals (e.g. Lu *et al.* 2014). Giant murines have been on the island since at least  
47  
48 187 the Middle Pleistocene (Louys *et al.* 2017), and likely constituted part of human diet until their  
49  
50 188 extinction (Glover, 1971).

51  
52  
53  
54  
55  
56 189

1  
2  
3 190 The ten specimens represented nine right femora and one left femur (**Figure 1**). The specimens  
4  
5 191 and associated thin sections are housed at the Department of Archaeology and Natural History,  
6  
7 192 and the School of Archaeology and Anthropology at the Australian National University  
8  
9 193 (Canberra, Australia) (see **Tables 1, 2** for accession numbers). For sampling consistency, the  
10  
11 194 femora were selected based on preservation, side, midshaft completeness for thin-sectioning,  
12  
13 195 and ensuring the final sample reflected a range of sizes. Bone histology and midshaft  
14  
15 196 measurements for two of the specimens (TDS0-30#4 and TDD1#11) have been previously  
16  
17 197 reported (Miszekiewicz *et al.* 2019). Most specimens were considered adult as indicated by  
18  
19 198 epiphyseal fusion and mature femoral form. However, some distal and proximal femoral ends  
20  
21 199 were fragmented. We also acknowledge that epiphyseal plate fusion in mammals cannot be  
22  
23 200 entirely relied on for age estimation (Geiger *et al.* 2014). Therefore, we supplemented the age  
24  
25 201 estimates from bone morphology with identification of adult tissue in bone microscopic  
26  
27 202 organisation. For the small specimens, bone histology was very similar to that of adult Wistar  
28  
29 203 rat (*Rattus norvegicus*) femoral cortex (see Singh & Gunberg, 1971; Martiniaková *et al.* 2005;  
30  
31 204 Sengupta, 2013; Miszekiewicz *et al.* 2019). One of the giant femora (TDS0-30#4) also showed  
32  
33 205 evidence of adult Haversian tissue (Miszekiewicz *et al.*, 2019).  
34  
35  
36  
37  
38  
39  
40  
41

## 42 207 **Femoral measurements**

43  
44 208 We quantitatively describe the size of each femur and compare them to a series of Asia-Pacific  
45  
46 209 rodent species of known weight (**Table 2**). Two variables could be consistently applied across  
47  
48 210 the specimens: femur midshaft width in a medial-lateral plane (MLW), and femur midshaft  
49  
50 211 depth in a cranial-caudal (CCD) plane (in mm). These were taken using standard digital  
51  
52 212 callipers (Mitutoyo®). The midshaft was either identified by dividing the length of intact  
53  
54 213 femora in half, or by locating shaft segments immediately distal to the third trochanter (dashed

1  
2  
3 214 line in **Figure 1A**). We report maximum length and femoral head diameter where possible  
4  
5 215 (**Table 1**), but exclude them from the statistical analyses as they represent only a fraction of  
6  
7  
8 216 our sample size. We computed body mass estimates using the femoral midshaft measurements.  
9  
10 217 Because this assemblage was commingled and only isolated dental remains were uncovered, a  
11  
12 218 confident match between postcranial and cranial elements per individual is not possible. In  
13  
14 219 addition to the fragmentation of the femora, this meant that we were unable to apply published  
15  
16 220 body mass estimation methods as they include dental data or they do not consider midshaft  
17  
18 221 diameters only as proxies (e.g. Moncunill-Solé *et al.* 2014). Furthermore, as our material is of  
19  
20 222 SEA origin, it warranted the calculation of new, region specific new body mass regression  
21  
22 223 equations based on our new data.  
23  
24  
25

26 224

### 28 225 **Thin section preparation and bone histology imaging**

30 226 Standard histological methods for fossil bone were followed to produce thin sections from each  
31  
32 227 femoral midshaft (Chinsamy & Raath, 1992; Miskiewicz *et al.* 2019). Femora were embedded  
33  
34 228 in Buehler® epoxy resin and cut at midshaft in a transverse plane using a Kemet MICRACUT®  
35  
36 229 151 Precision Cutter with a diamond cutting blade. Samples were then glued to microscope  
37  
38 230 slides using Araldite®, ground and polished on a series of pads and cloths, dehydrated in  
39  
40 231 ethanol (95% and 100%) baths, cleared in xylene, and cover slipped using a DPX mounting  
41  
42 232 medium. The resulting sections were approximately 100-150 µm thick.  
43  
44  
45

46 233

48  
49 234 Micro-anatomical descriptions indicate that rat compact bone is mostly avascular, marked with  
50  
51 235 radial canals, osteocytes residing within osteocyte lacunae (Martiniaková *et al.* 2005; Oršolić  
52  
53 236 *et al.* 2018). Haversian, remodelled, tissue in murine bone has been reported only in a few case  
54  
55 237 studies (Kolb *et al.* 2015; Miskiewicz *et al.* 2019). As osteocytes are responsible for bone

58 Miskiewicz et al BJLS R2 Page 11 of 37

1  
2  
3 238 maintenance, they essentially sustain living tissue by signalling mechanical load and  
4  
5 239 facilitating the exchange of nutrients (Han *et al.* 2004; Tate *et al.* 2004). Osteocytes are the  
6  
7 240 most abundant bone cell found in vertebrates (Hall, 2015), and as much as the cells themselves  
8  
9 241 do not typically preserve in fossil bone, the cavities they would have resided in do. Osteocyte  
10  
11 242 lacunae in fossil or archaeological bone can thus be studied as a proxy for osteocyte  
12  
13 243 proliferation and bone metabolism (Bromage *et al.* 2009; Hogg *et al.* 2017; Miskiewicz, 2016;  
14  
15 244 Miskiewicz & Mahoney, 2017). We accessed these micro-features from each thin section  
16  
17 245 using standard light microscopy (Olympus BX51 and BX53 microscope with a DP73 and DP74  
18  
19 246 camera respectively) and analysed them in ImageJ® (1.51k 2013).  
20  
21  
22  
23  
24  
25

26 248 All sections were first imaged at a 40x total magnification (~6.07 mm<sup>2</sup> each image) so that an  
27  
28 249 overview micrograph for each sample could be produced. For the larger femoral sections, an  
29  
30 250 average of 10-14 individual images were collected, whereas the smaller femora were easily  
31  
32 251 reproduced from two to three individual images. Each of these were stitched manually in Adobe  
33  
34 252 Photoshop CC 2014 to create a starting point from which to identify the best preserved and  
35  
36 253 taphonomy/bio-erosion free region of interest (ROI). Unlike modern or fresh bone, the  
37  
38 254 palaeontological context of our samples meant that there was incomplete and inconsistent  
39  
40 255 preservation of microstructure. Therefore, the selection of ROIs for data collection was  
41  
42 256 determined by the visibility of, and our confidence in identifying, osteocyte lacunae. Where  
43  
44 257 possible, we selected the same anatomical aspect of each femur so that osteocyte lacunae data  
45  
46 258 could be compared consistently across the whole sample. This resulted in isolating the lateral  
47  
48 259 femur region with some caudal or cranial overlap (**Figure 1B**). Ultimately, we captured  
49  
50 260 osteocyte lacunae data from one ROI per section at 100x total magnification representing an  
51  
52 261 image that measures ~0.93 mm<sup>2</sup>. The bone area within each image ranged from ~0.93 mm<sup>2</sup> in  
53  
54  
55  
56  
57  
58  
59  
60

Miskiewicz et al BJLS R2 Page 12 of 37

1  
2  
3 262 the giant rats to  $\sim 0.35 \text{ mm}^2$  in the smaller rats. In the latter case, the area of the bone itself was  
4  
5 263 measured by directly tracing the bone tissue, excluding image regions that were empty. Using  
6  
7 264 the MultiPoint tool in ImageJ® (1.51k 2013), osteocyte lacunae were first recorded as total  
8  
9 265 counts from the most superior surface of each section. Prior to counting, all images were  
10  
11 266 adjusted to grey scale (black and white intensity = 100) and then exposed (offset = -0.100) in  
12  
13 267 Adobe Photoshop CC 2014 to enhance each lacuna so that they could be distinguished against  
14  
15 268 the white background (**Figure 1B**). In order to estimate densities, a standard Ot.Dn (osteocyte  
16  
17 269 lacunae density = osteocyte lacunae count/ section area in  $\text{mm}^2$ ) variable was created by  
18  
19 270 dividing each osteocyte lacunae count by the bone area examined in  $\text{mm}^2$  (Li *et al.* 2011;  
20  
21 271 Miszkiewicz, 2016). To check for potential observer bias, osteocyte lacunae in two randomly  
22  
23 272 selected images from our image bank were independently scored by three observers – two  
24  
25 273 authors of the present study (JM, JL), and one external histologist (TJ Stewart).  
26  
27  
28  
29  
30  
31  
32

### 33 275 **Statistical analyses**

34  
35 276 All statistical analyses were conducted in IBM SPSS Statistics 22.0 (2013), Past3 (Hammer *et*  
36  
37 277 *al.*, 2001), and R 3.6.0. We split the analyses into two steps – 1) testing for a phylogenetic  
38  
39 278 signal and creating body mass regressions, 2) assessing relationships between measures of body  
40  
41 279 size and Ot.Dn by examining linear trends and testing for allometric changes (Kilmer &  
42  
43 280 Rodríguez, 2017). As we only had three independent data points, inter-observer measurements  
44  
45 281 were compared between the repeated data descriptively by assessing the extent of deviation  
46  
47 282 from the mean. The measurements were deemed repeatable if the disagreement was  $< 0.05\%$ .  
48  
49  
50

51 283

52 284

53 285

1  
2  
3 286 **1) Phylogenetic signal and body mass regressions**  
4

5 287 To produce a body mass regression equation that could be used to estimate body mass for our  
6  
7 288 Timorese specimens, we collected CCD and MLW measurements for specimens of known  
8  
9  
10 289 body mass for 17 Asia-Pacific murine species (**Table 2**). Where data were available for  
11  
12 290 multiple specimens of the same species, these were combined to produce mean estimates for  
13  
14 291 that species (**Table 2**). The final CCD and MLW measurements and body mass for each species  
15  
16 292 were natural-logged (ln) transformed prior to analysis. We used a phylogenetic generalised  
17  
18 293 least squares (PGLS) approach (Symonds & Blomberg, 2014), with uncertainty in phylogenetic  
19  
20 294 relationships and divergence times among our species taken into account using the R package  
21  
22 295 sensiPhy (Paterno *et al.* 2018) and 1000 trees from the “Phylacine” database (Faurby *et al.*  
23  
24 296 2018), pruned to match our set of 17 species using the “keep.tip” function of the R package  
25  
26 297 ape (Paradis & Schliep, 2019). We used the “physig” function of sensiPhy to calculate the  
27  
28 298 maximum likelihood estimate of Pagel’s lambda ( $\lambda$ ) in the residuals of our data as a measure  
29  
30 299 of phylogenetic signal, and then used this value of  $\lambda$  to determine the best-fitting regression.  
31  
32 300 We calculated three different regressions, using body mass and either: 1) CCD, 2) MLW, or 3)  
33  
34 301 cross-sectional area of the femoral midshaft, which we calculated as  $\pi \times (0.5 \times \text{CCD}) \times (0.5 \times$   
35  
36 302  $\text{MLW})$ , i.e., treating it as an ellipse. We then used the Akaike Information Criterion (AIC) to  
37  
38 303 determine which of these three regressions showed the best fit to our data, and used the best-  
39  
40 304 fitting regression to estimate body mass for our Timorese specimens.  
41  
42  
43  
44  
45  
46  
47  
48

49 306 **2) Evaluating relationships between femur size, body mass, and osteocyte lacunae**

50  
51 307 Firstly, all the raw data for body mass estimates (g), CCD (mm), MLW (mm), and Ot.Dn were  
52  
53 308 correlated using non-parametric Spearman’s *Rho* tests to assess linear agreements between  
54  
55 309 data. These were repeated on the raw Ot.Dn data corrected by femur midshaft size  
56  
57

1  
2  
3 310 (Ot.Dn/MLW and Ot.Dn/CCD). The results from these correlations were interpreted following  
4  
5 311 Taylor (1990), whereby  $Rho > 0.67$  is considered a high or strong correlation. To assess  
6  
7 312 allometric changes in Ot.Dn along with femur size and body mass estimates we used ordinary  
8  
9 313 least squares regressions (OLS) on log10 transformed data (which decreased data variability).  
10  
11 314 We interpret the  $r^2$ , slope ( $b$ ), confidence interval (CI), intercept ( $Y$ ), and statistical significance  
12  
13 315 of these models using uncorrected  $p$  as well as Bonferroni corrected (uncorrected  $p$  divided by  
14  
15 316 the number of repeated tests), more conservative,  $p$  for each set of analysis. Plots fitting OLS  
16  
17 317 regressions illustrate the trend line and CIs to visually describe the scatter of data.  
18  
19  
20  
21  
22  
23

## 24 319 RESULTS

25  
26 320 There was no inter-observer error in the independent measurements, with the three observers  
27  
28 321 providing almost equal counts of lacunae per image (image 1 mean 127.33, SD 2.08, similarity  
29  
30 322 = 98.37%; image 2 mean 132.67, SD = 2.52, similarity = 98.10%). The largest midshaft femur  
31  
32 323 measured 7.25 mm in MLW and 5.89 mm in CCD, respectively (**Tables 1-3**). The smallest  
33  
34 324 examined femur was of 2.33 mm MLW and 1.98 mm CCD, respectively (Miskiewicz *et al.*,  
35  
36 325 2019). Body mass estimates for the sample ranged from 75g in the smallest specimen to 1188g  
37  
38 326 in the largest specimen. We incorporated these estimates (relying on MLW and CCD data) into  
39  
40 327 a bar chart encompassing modern rat data of known weight (**Figure 2, Table 2**). This shows  
41  
42 328 that the smaller fossil murines were likely similar in their body mass to a house mouse (*Mus*  
43  
44 329 *domesticus*), whereas the giant murines may have been comparable to a subalpine woolly rat  
45  
46 330 (*Mallomys istapantap*, up to 2 kg in weight).  
47  
48  
49  
50  
51  
52  
53  
54  
55  
56  
57  
58  
59  
60



### 334 **Body mass estimates**

335 The phylogenetic signal (measured by Pagel's lambda) in our data for specimens of known  
336 body mass for 17 Asia-Pacific species (**Table 2**) was very low and non-significant (mean =  
337 0.03, CI = 0.02, CI = 0.04,  $p = 0.99$ ). AIC values for our three regressions were as follows:  
338  $\ln(\text{MLWfemur width}) = 10.38$ ,  $\ln(\text{CCDfemur depth}) = 16.53$ ,  $\ln(\text{femoral midshaft cross-}$   
339  $\text{sectional areafemur area}) = 8.59$ . As lower AIC values represent better model fit, it is clear that  
340 combining femur width and depth into an estimate of femur area resulted in a better fitting  
341 model. The PGLS regression for  $\ln(\text{femur area})$  and an the maximum likelihood (ML) estimate  
342 of Pagel's lambda ( $\lambda = 0.03$ ) was:

$$343 \quad \ln(\text{body mass}) = 1.24 \times \ln[(\text{femur area} = \pi \times (0.5 \times \text{CCD}) \times (0.5 \times \text{MLW}))] + 2.724$$

344 Body mass estimates for the Timor specimens, based on the above equation, are reported in  
345 **Table 2**.

### 347 **Osteocyte lacunae densities**

348 Osteocyte lacunae density data ranged from 2483.21/mm<sup>2</sup> minimum to 3936.32/mm<sup>2</sup>  
349 maximum. However, corrections by femur size adjusted the data to 342.51/mm<sup>2</sup> and  
350 1499.30/mm<sup>2</sup> range in the MLW category, and 421.60/mm<sup>2</sup> to 1764.32/mm<sup>2</sup> in the CCD  
351 measure of femur shaft (**Tables 1-3**). The results of Spearman's *Rho* tests (**Table 4**) suggest  
352 that Ot.Dn data are in strongly negative and statistically significant relationships with measures  
353 of femur size and body mass estimates. The *Rho* achieved in these cases was -0.952 to -0.661  
354 with  $p < 0.05$ . However, when CCD was considered, these relationships were not consistent,  
355 whereby *Rho* was -0.576 ( $p = 0.082$ ) when raw Ot.Dn were included in the analysis. When  
356 using a more conservative Bonferroni correction on repeated tests, the correlation between

1  
2  
3 357 estimated body mass, and MLW and raw Ot.Dn did not meet significance, with  $p = 0.038$  and  
4  
5 358 0.019 respectively.  
6  
7  
8 359

9  
10 360 Ordinary least squares regression of all log transformed data resulted in an almost consistently  
11  
12 361 statistically significant and strong models that showed negative allometry (**Table 4**). Two of  
13  
14 362 the models - log(estimated body mass), log(CCD), and log(Ot.Dn), returned  $p > 0.05$  and had  
15  
16 363 weak  $r^2$ . However, most of the models were statistically significant at  $\alpha = 0.05$ , except for  
17  
18 364 Bonferroni corrected log(MLW) and log(Ot.Dn) where  $0.05 > p > 0.017$ . The data scatter  
19  
20 365 around regression lines was wider in the cases where raw data are used, but better fitting models  
21  
22 366 can be seen for those where the size of the femur is accounted for in Ot.Dn (**Figure 3**).  
23  
24  
25  
26 367

## 27 28 368 **DISCUSSION**

29  
30 369 Our analyses revealed statistically significant negative correlations, and an allometric  
31  
32 370 relationship between the histological and macroscopic measures of bone metabolism and body  
33  
34 371 mass in a range of giant and small fossil murine rodents from Timor Island. Collectively, these  
35  
36 372 provide clear evidence that fossil murine gigantism was associated with a slowing down of  
37  
38 373 bone metabolism as inferred from low osteocyte lacunae densities. In contrast, the smaller  
39  
40 374 murines in our sample exhibit increased osteocyte lacunae densities, indicating accelerated  
41  
42 375 bone metabolism. Our study has implications for current understanding of the evolution of  
43  
44 376 mammalian bone physiology in relation to body mass and insularity, as well as the  
45  
46 377 palaeoenvironments of Timor.  
47  
48  
49  
50

51 378

52 379

53 380

1  
2  
3 381 **Bone metabolism**  
4

5 382 This study unlocks bone physiology from cell structures preserved in thin sections of fossil  
6  
7 383 femora to understand the biological adaptation of Timorese island members of the rodent  
8  
9  
10 384 subfamily Murinae, and to examine the relationships between bone osteocyte lacunae densities  
11  
12 385 and body mass when compared between these in mammalian species. We have previously  
13  
14 386 shown changes in osteocyte lacunae densities can be linked to bone remodelling rates (e.g.  
15  
16 387 Miskiewicz, 2016), and as such can provide insights into bone metabolism fluctuations. When  
17  
18 388 examined within living mammals, strong inverse correlations between Ot.Dn and body mass  
19  
20 389 show that osteocyte proliferation corresponds to body mass (Hogg *et al.* 2017). Data presented  
21  
22 390 here support these ideas as they demonstrate a strongly negative decline in Ot.Dn with  
23  
24 391 increasing within Timorese island murines. These data are similar to previous inter-specific  
25  
26 392 findings for extant non-primate mammals (Mullender *et al.* 1996), and to those described by  
27  
28 393 Bromage *et al.* (2009) for species that included adult pygmy (*Phanourios minutus*) and common  
29  
30 394 hippo (*Hippopotamus amphibius*), as well as the Mohol bushbaby (lesser galagos, *Galago*  
31  
32 395 *moholi*) and greater dwarf lemur (*Cheirogales major*) (Bromage *et al.*, 2009: 393). A pygmy  
33  
34 396 hippo of an approximate 200 kg body mass had an average Ot.Dn reported as 23,641/mm<sup>3</sup>,  
35  
36 397 whereas its larger counterpart (*H. amphibius*) had an Ot.Dn of 16,667/mm<sup>3</sup>. In the same study,  
37  
38 398 an adult lesser galago with an approximate 244 g weight had 51,724/mm<sup>3</sup> Ot.Dn, which was  
39  
40 399 much higher than the 31,526/mm<sup>3</sup> Ot.Dn from a greater galago with a body weight of 400 g.  
41  
42 400 Our data conform to this general pattern. Our study shows a much more widely dispersed  
43  
44 401 osteocyte lacunae in the giant murine specimen when compared to its smaller counterpart  
45  
46 402 (**Figure 1C**), and body size and Ot.Dn are related through negative allometry.  
47  
48  
49  
50  
51  
52  
53  
54 403

1  
2  
3 404 Bone histology limitations of our study pertain to being understood two-dimensionally only,  
4  
5 405 whereas three-dimensional scans of each entire femur in the sample may yield more osteocyte  
6  
7 406 lacunae data in the future. We are also unable to make further connections to energy variables,  
8  
9 407 such as the BMR, because of the nature of the samples. With no direct measures of muscle or  
10  
11 408 physical activity in our fossil murine sample, we are limited in understanding how their  
12  
13 409 energetic expenditure and heat generation may have fitted into life history strategies (McNab,  
14  
15 410 2019). Finally, the unknown species identification limited our interpretations of the Ot.Dn links  
16  
17 411 with phylogeny. However, previous accounts of inter-specific variation in bone micro-  
18  
19 412 organisation have cited animal size and lifespan as more direct influences on histology than  
20  
21 413 phylogeny (de Ricqlès, 1993; Greenlee & Dunnell, 2010).  
22  
23  
24  
25  
26  
27  
28

#### 29 415 **The extinct giant murines of Timor**

30 416 As predicted by the island rule, animals may change with response to insular environments due  
31  
32 417 to selective pressures that encourage anatomical and behavioural modifications. Smaller,  
33  
34 418 lighter, and faster growing mammals can adapt more easily than those that have increased  
35  
36 419 energetic demands. While being smaller comes with many advantages, it also decreases  
37  
38 420 longevity as outlined in the classic r and K-selection evolutionary strategy principles (Pianka,  
39  
40 421 1970). The relatively slow bone metabolism of giant Timorese murines could indicate extended  
41  
42 422 lifespans, which can be linked to favourable palaeoenvironments.  
43  
44  
45  
46  
47  
48

49 424 It is extremely difficult to pinpoint specific casualty of our giant murine extinction as multiple  
50  
51 425 factors must have played a role in their demise. However, when compared to prior  
52  
53 426 palaeobiological models that test extinction causality in small mammals in islands (e.g. Bover  
54  
55 427 & Alcover, 2008), we can at least propose some environmental extinction elements. For

1  
2  
3 428 example, Bover and Alcover (2008) examined the extinction of Mallorcan small mammals  
4  
5 429 analysing climate, predation, competition, habitat loss/ modification, and anthropogenic factors  
6  
7  
8 430 as potential reasons driving extinction in the Western Mediterranean. The authors obtained  
9  
10 431 radiocarbon ages from fossil bone collagen to reconstruct uncertainty and restricted periods of  
11  
12 432 extinction for species of Balearic dormouse (*Eliomys morpheus*) and the Balearic shrew  
13  
14 433 (*Asoriculus hidalgo*), and corroborated archaeological and direct dating data of introduced  
15  
16 434 garden dormouse *Eliomys quercinus* and the wood mouse *Apodemus sylvaticus*. They  
17  
18  
19 435 concluded that the extinction of the Mallorcan small mammals would have been most likely  
20  
21 436 indirectly caused by human activity (the spread of disease). For the giant murines of Timor, we  
22  
23 437 can find supporting evidence in the historical and archaeological record for at least two of these  
24  
25  
26 438 items – human co-existence with giant murines, and habitat modification on the island of  
27  
28  
29 439 Timor.

30 440  
31  
32  
33 441 Fossil evidence suggests that giant murines were in Timor from the Middle Pleistocene (Louys  
34  
35 442 *et al.* 2017), by which time the island was also home to small-bodied stegodons (*Stegodon*  
36  
37 443 '*trigonocephalus*' and *Stegodon timorensis*) - elephant-like animals that may have evolved into  
38  
39 444 pygmy forms on the island (Louys *et al.* 2016). This hints at the effect of insularity impacting  
40  
41 445 more than one mammal in Timor. To that end, giant murines have been found in association  
42  
43 446 with humans in Timor for more than 40,000 years (Hawkins *et al.* 2017). Glover (1971:177),  
44  
45 447 when reviewing archaeological and palaeontological excavations on the island of Timor since  
46  
47 448 about 1935, noted that giant murines would have been “the principal prey” (in addition to  
48  
49 449 pteropodid bats) of the first human groups. Increasing human contact may have not only  
50  
51 450 entailed predation: it would have also likely led to significant habitat alteration, introduction  
52  
53 451 of competitors, other predators, and disease.

Miszekiewicz et al BJLS R2 Page 20 of 37

1  
2  
3 452  
4

5 453 Human driven deforestation in SEA is a well-established issue that contributes to the reduction  
6  
7  
8 454 of resources and elimination forest ecology (see McWilliam, 2005; O'Connor *et al.* 2012).  
9  
10 455 Modern biodiversity conservation efforts have continually documented the disappearance of  
11  
12 456 rich native habitats in areas densely populated and exploited by humans in SEA (Sodhi *et al.*  
13  
14 457 2010; Hughes, 2017; Carlson *et al.* 2018). Historical annotations indicate that Timor became  
15  
16 458 an important centre for timber export of white sandalwood ca. 1500 AD (McWilliam, 2005;  
17  
18 459 O'Connor *et al.* 2012), with prior introduction of metal tools (bronze and iron) to island SEA  
19  
20 460 sometime 2500 and 1500 years ago (Higham, 1996; Bulbeck, 2008). These tool developments  
21  
22 461 would have facilitated effective slash-and-burn agriculture, with the later timber export activity  
23  
24 462 accelerating forest cultivation. By the Timorese fort building period, ~1500 years ago, many  
25  
26 463 small, but no giant murine fossils are recovered in excavations, suggesting extinction of the  
27  
28 464 latter by this time (O'Connor & Aplin, 2007)..  
29  
30  
31  
32

33 465  
34

35 466 While more direct evidence for the Timor palaeoenvironments, and a larger sample size, is  
36  
37 467 needed, our histology study suggests that the slower bone metabolism of giant murines fitted  
38  
39 468 principles of gigantism under the island rule. They may have been associated with slower  
40  
41 469 growth and maturation requiring relatively higher amounts of energy obtained from good  
42  
43 470 quality or quantity of resources, low levels of predation, facilitating longevity and increased  
44  
45 471 offspring quality (Reznick *et al.* 2002; Dammhahn *et al.* 2018). Our findings match those from  
46  
47 472 another palaeohistology study that inferred an “exceptionally long lifespan” (Orlandi-Oliveras  
48  
49 473 *et al.* 2016: 238) from bone histology in a giant fossil glirid rodent, *Hypnomys onicensis*, on  
50  
51 474 the Balearic Islands, confirming slower life history in an insular context. We acknowledge that  
52  
53 475 true “gigantism” of our specimens cannot be confirmed until we know the body mass of their  
54  
55  
56  
57  
58  
59  
60

Miszkievicz et al BJLS R2 Page 21 of 37

1  
2  
3 476 ancestors and have an accurate phylogeny. The island rule specifies that if a colonising  
4  
5 477 ancestral species was initially small, and the newly colonised island marked with favourable  
6  
7 478 habitats, evolving into a giant form would be selectively advantageous. While we know that  
8  
9 479 Timor has never been connected to SEA or Australia, and thus has been truly geographically  
10  
11 480 isolated throughout its history, cases of island rodents that evolved into dwarfed from larger  
12  
13 481 forms following deterioration in food resources are known (Durst & Roth, 2015).  
14  
15

## 16 17 482 **CONCLUSIONS**

18  
19 483 Lab rats have long been used in biology research, letting us observe animal phenotypic change  
20  
21 484 upon experimental modification of external environmental and internal genotypic conditions.  
22  
23 485 Here, we conducted an experiment in deep time, assessing murine size and bone microanatomy  
24  
25 486 in the context of a changing and insular environment. The gradient of murine size in this sample  
26  
27 487 served as a platform for investigating links between bone metabolism and its response to  
28  
29 488 insularity. We show that the now extinct giant murines of Timor were likely characterised by  
30  
31 489 slow bone metabolism, which could be related to abundant resources and plentiful forests until  
32  
33 490 human driven action destroyed these habitats. This finding is consistent with predictions made  
34  
35 491 from the island rule. We also find that surviving smaller murines were equipped with faster  
36  
37 492 bone metabolism, allowing them to survive less certain environmental contexts once  
38  
39 493 anthropogenic alteration increased. These findings further our understanding of vertebrate bone  
40  
41 494 tissue metabolism, its adaptation in response to ecological change, along with its versatility and  
42  
43 495 plasticity that can be reconstructed at a microscopic level.  
44  
45  
46  
47  
48

## 49 496 **ACKNOWLEDGMENTS**

50 497  
51 498 Shimona Kealy selected murine specimens for this experiment. Tahlia Stewart participated in  
52  
53 499 the inter-observer error test. Fieldwork in Timor and subsequent analysis of specimens were  
54  
55 500  
56  
57

1  
2  
3 501 undertaken with permissions from the Director General of Culture, Mrs Cecilia Assis, Ministry  
4  
5 502 of Tourism, Art and Culture, Timor-Leste. Research funding was received from the Australian  
6  
7 503 Research Council (LF120100156 to O'Connor, FT160100450 to Louys, DE190100068 to  
8  
9 504 Miskiewicz). We thank three anonymous reviewers, Blanca Moncunill-Solé, and John A.  
10  
11 505 Allen for feedback and constructive suggestions that greatly improved this manuscript. We are  
12  
13 506 grateful to Kristofer Helgen for advice on specimen accessioning. We dedicate this paper to  
14  
15 507 the late Ken Aplin.  
16  
17  
18  
19 508

For Peer Review



1  
2  
3 509 **REFERENCES**

- 4  
5 510 Abdelkrim J, Pascal M, Samadi S. 2005. Island colonization and founder effects: the invasion  
6  
7 511 of the Guadeloupe islands by ship rats (*Rattus rattus*). Mol Ecol 14: 2923-2931.  
8  
9  
10 512 Adler GH. 1996. The island syndrome in isolated populations of a tropical forest rodent.  
11  
12 513 Oecologia 108: 694-700.  
13  
14  
15  
16 514 Adler GH, Levins R. 1994. The island syndrome in rodent populations. Q Rev Biol 69: 473-  
17  
18 515 490.  
19  
20  
21 516 Aplin KP, Helgen KM. 2010. Quaternary murid rodents of Timor Part I: new material of  
22  
23 517 *Coryphomys buehleri* Schaub, 1937, and description of a second species of the genus. Bull Am  
24  
25 518 Mus Nat 341: 1-80.  
26  
27  
28  
29 519 Benton MJ, Csiki Z, Grigorescu D, Redelstorff R, Sander PM, Stein K, Weishampel D. B.  
30  
31 520 2010. Dinosaurs and the island rule: The dwarfed dinosaurs from Hațeg Island. Palaeogeogr  
32  
33 521 Palaeoclimatol Palaeoecol 293: 438-454.  
34  
35  
36  
37 522 Boback SM, Guyer C. 2003. Empirical evidence for an optimal body size in snakes. Evol 57,  
38  
39 523 345-351.  
40  
41  
42 524 Bocherens H, Michaux J, Talavera FG, van der Plicht J. 2006. Extinction of endemic  
43  
44 525 vertebrates on islands: the case of the giant rat *Canariomys bravori* (Mammalia, Rodentia) on  
45  
46 526 Tenerife (Canary Islands, Spain). C R Palevol 5: 885-91.  
47  
48  
49  
50 527 Bover P, Alcover JA. 2008. Extinction of the autochthonous small mammals of Mallorca  
51  
52 528 (Gymnesic Islands, Western Mediterranean) and its ecological consequences. J Biogeogr 35:  
53  
54 529 1112-1122.  
55  
56  
57

- 1  
2  
3 530 Bromage TG, Lacruz RS, Hogg R, Goldman HM, McFarlin SC, Warshaw J, Dirks W, Perez-  
4  
5 531 Ochoa A, Smolyar I, Enlow DH, Boyde A. 2009. Lamellar bone is an incremental tissue  
6  
7 532 reconciling enamel rhythms, body size, and organismal life history. *Calcif Tissue Int* 84: 388-  
8  
9 533 404.  
10  
11  
12  
13 534 Brown JH, Kodric-Brown A. 1977. Turnover rates in insular biogeography: effect of  
14  
15 535 immigration on extinction. *Ecol* 58: 445-449.  
16  
17  
18 536 Brown JH, Sibly RM. 2006. Life-history evolution under a production constraint. *Proc Natl*  
19  
20 537 *Acad Sci* 103: 17595-17599.  
21  
22  
23  
24 538 Bulbeck D. 2008. An integrated perspective on the Austronesian diaspora: The switch from  
25  
26 539 cereal agriculture to maritime foraging in the colonisation of Island Southeast Asia. *Aus*  
27  
28 540 *Archaeol* 67: 31-51.  
29  
30  
31 541 Carlson KM, Heilmayr R, Gibbs HK, Noojipady P, Burns DN, Morton DC, Walker NF, Paoli  
32  
33 542 GD, Kremen C. 2018. Effect of oil palm sustainability certification on deforestation and fire in  
34  
35 543 Indonesia. *Proc Natl Acad Sci* 115: 121-6.  
36  
37  
38  
39 544 Chinsamy A, Raath MA. 1992. Preparation of fossil bone for histological examination.  
40  
41 545 *Palaeont Afr* 29: 39 – 44.  
42  
43  
44  
45 546 Chinsamy-Turan A. 2011. *Forerunners of mammals: radiation, histology, biology.*  
46  
47 547 Bloomington, US: Indiana University Press.  
48  
49  
50 548 Clegg SM, Owens PF. 2002. The ‘island rule’ in birds: medium body size and its ecological  
51  
52 549 explanation. *Proc R Soc Lond B Biol Sci* 269: 1359-1365.  
53  
54  
55  
56  
57  
58  
59  
60

- 1  
2  
3 550 Dammhahn M, Dingemanse NJ, Niemelä PT, Réale D. 2018. Pace-of-life syndromes: a  
4  
5 551 framework for the adaptive integration of behaviour, physiology and life history. *Behav Ecol*  
6  
7 552 *Sociobiol* 72: 62.
- 8  
9  
10  
11 553 Darwin C. 1859. *The Origin of Species by Means of Natural Selection: Or, The Preservation*  
12  
13 554 *of Favored Races in the Struggle for Life*. London, UK: Murray.
- 14  
15  
16 555 de Ricqlès AJ. 1993. Some remarks on palaeohistology from a comparative evolutionary point  
17  
18 556 of view. In: Grupe G, Garland AN, eds: *Histology of ancient human bone: methods and*  
19  
20 557 *diagnosis*. Berlin: Springer, 37-77.
- 21  
22  
23  
24 558 de Ricqlès AJ. 2011. Vertebrate palaeohistology: Past and future. *C R Palevol* 10: 509-515.
- 25  
26  
27 559 Durst PA, Roth VL. 2015. Mainland size variation informs predictive models of exceptional  
28  
29 560 insular body size change in rodents. *P Roy Soc B-Biol Sci* 282: 20150239.
- 30  
31  
32  
33 561 Enlow DH, Brown SO. 1956. A comparative histological study of fossil and recent bone  
34  
35 562 tissues. Part I. *Tex J Sci* 8: 405-443.
- 36  
37  
38 563 Enlow DH, Brown SO. 1957. A comparative histological study of fossil and recent bone  
39  
40 564 tissues. Part II. *Tex J Sci* 9: 186-214.
- 41  
42  
43 565 Enlow DH, Brown SO. 1958. A comparative histological study of fossil and recent bone  
44  
45 566 tissues. *Tex J Sci* 10: 187-230.
- 46  
47  
48  
49 567 Faurby S, Davis M, Pedersen RO, Schowanek SD, Antonelli A, Svenning JC. 2018.  
50  
51 568 *PHYLACINE 1.2: The Phylogenetic atlas of mammal macroecology*. *Ecology* 99: 2626.
- 52  
53  
54 569 Faurby S, Svenning J-C. 2016. Resurrection of the island rule: human-driven extinctions have  
55  
56 570 obscured a basic evolutionary pattern. *Am Nat* 187: 812–820.

Miszkievicz et al BJLS R2 Page 26 of 37

- 1  
2  
3 571 Firmat C, Rodrigues HG, Hutterer R, Rando JC, Alcover JA, Michaux J. 2011. Diet of the  
4  
5 572 extinct Lava mouse *Malpaisomys insularis* from the Canary Islands: insights from dental  
6  
7 573 microwear. *Naturwiss* 98: 33-7.
- 8  
9  
10 574 Firmat C, Rodrigues HG, Renaud S, Hutterer R, Garcia-Talavera Fr, Michaux J. 2010.  
11  
12 575 Mandible morphology, dental microwear, and diet of the extinct giant rats *Canariomys*  
13  
14 576 (Rodentia: Murinae) of the Canary Islands (Spain). *Biol J Linn Soc* 101: 28-40.
- 15  
16  
17 577 Foster JB. 1964. Evolution of mammals on islands. *Nature* 202: 234-235.
- 18  
19  
20  
21 578 Geffen E, Yom-Tov Y. 2019. Pacific island invasions: how do settlement time, latitude, island  
22  
23 579 area and number of competitors affect body size of the kiore (Polynesian rat) across the  
24  
25 580 Pacific?. *Biol J Linn Soc* 126: 462–470.
- 26  
27  
28  
29 581 Geiger M, Forasiepi AM, Koyabu D, Sánchez-Villagra MR. 2014. Heterochrony and post-natal  
30  
31 582 growth in mammals—an examination of growth plates in limbs. *J Evo Biol* 27: 98-115.
- 32  
33  
34  
35 583 Glover IC. 1971. Prehistoric research in Timor. In: Mulvaney DJ, Golson J, eds: *Aboriginal*  
36  
37 584 *man and environment in Australia*. Canberra: Australian National University Press, 154-181.
- 38  
39  
40 585 Greenlee DM, Dunnell RC. 2010. Identification of fragmentary bone from the Pacific. *J*  
41  
42 586 *Archaeol Sci* 37: 957-970.
- 43  
44  
45  
46 587 Hall BK. 2015. *Bones and cartilage: developmental and evolutionary skeletal biology*. London,  
47  
48 588 UK: Elsevier Academic Press.
- 49  
50  
51 589 Hammer Ø, Harper DAT, Ryan PD. 2001. PAST-palaeontological statistics, ver. 1.89. *Palaeont*  
52  
53 590 *Electr* 4: 1–9.
- 54  
55  
56  
57  
58  
59  
60

- 1  
2  
3 591 Han Y, Cowin SC, Schaffler MB, Weinbaum S. 2004. Mechanotransduction and strain  
4  
5 592 amplification in osteocyte cell processes. *Proc Natl Acad Sci* 101: 16689-94.  
6  
7  
8 593 Harper GA, Dickinson KJ, Seddon PJ. 2005. Habitat use by three rat species (*Rattus* spp.) on  
9  
10 594 Stewart Island/Rakiura, New Zealand. *N Z J Ecol* 29: 251-260.  
11  
12  
13  
14 595 Hawkins S, O'Connor S, Maloney TR, Litster M, Kealy S, Fenner JN, Aplin K, Boulanger C,  
15  
16 596 Brockwell S, Willan R, Piotto E. Oldest human occupation of Wallacea at Laili Cave, Timor-  
17  
18 597 Leste, shows broad-spectrum foraging responses to late Pleistocene environments. *Quaternary*  
19  
20 598 *Sci Rev* 171: 58-72.  
21  
22  
23  
24 599 Higham C. 1996. *The Bronze Age of Southeast Asia*. Cambridge, UK: Cambridge University  
25  
26 600 Press.  
27  
28  
29 601 Hogg RT, Bromage TG, Goldman HM, Katris JA, Clement JG. 2017. The Havers–Halberg  
30  
31 602 oscillation and bone metabolism. In: Percival CJ, Richtsmeier, JT. *Building bones: bone*  
32  
33 603 *formation and development in anthropology*. Cambridge, UK: Cambridge University Press. pp.  
34  
35 604 254-280.  
36  
37  
38  
39 605 Hughes AC. 2017. Understanding the drivers of Southeast Asian biodiversity loss. *Ecosphere*  
40  
41 606 8: e01624.  
42  
43  
44  
45 607 Itescu Y, Karraker NE, Raia P, Pritchard PC, Meiri S. 2014. Is the island rule general? Turtles  
46  
47 608 disagree. *Glob Ecol Biogeogr* 23: 689-700.  
48  
49  
50 609 Kawamura Y. 1991. Quaternary mammalian faunas in the Japanese Islands. *Quaternary Res*  
51  
52 610 (*Daiyonki-Kenkyu*) 30: 213-220.  
53  
54  
55  
56  
57  
58  
59  
60

- 1  
2  
3 611 Kilmer JT, Rodríguez RL. 2017. Ordinary least squares regression is indicated for studies of  
4  
5 612 allometry. *J Evol Biol* 30: 4-12.  
6  
7  
8  
9 613 Kolb C, Scheyer TM, Veitschegger K, Forasiepi AM, Amson E, van der Geer AA, van den  
10  
11 614 Hoek Ostende LW, Hayashi S, Sánchez-Villagra MR. 2015. Mammalian bone palaeohistology:  
12  
13 615 a survey and new data with emphasis on island forms. *PeerJ* 22: e1358.  
14  
15  
16 616 Köhler M. 2010. Fast or slow? The evolution of life history traits associated with insular  
17  
18 617 dwarfing. In: Pérez-Mellado V, Ramon C, eds: *Islands and evolution*, Mallorca, Spain: Institut  
19  
20 618 Menorquí d'Estudis Recerca, 261-280.  
21  
22  
23  
24 619 Köhler M, Marín-Moratalla N, Jordana X, Aanes R. 2012. Seasonal bone growth and  
25  
26 620 physiology in endotherms shed light on dinosaur physiology. *Nature* 487: 358.  
27  
28  
29 621 Köhler M, Moyà-Solà S. 2009. Physiological and life history strategies of a fossil large  
30  
31 622 mammal in a resource-limited environment. *Proc Natl Acad Sci* 106: 20354-20358.  
32  
33  
34  
35 623 Lawlor TE. 1982. The evolution of body size in mammals: evidence from insular populations  
36  
37 624 in Mexico. *Am Nat* 119: 54-72.  
38  
39  
40 625 Li ZC, Jiang SD, Yan J, Jiang LS, Dai LY. 2011. Small-animal PET/CT assessment of bone  
41  
42 626 microdamage in ovariectomized rats. *J Nucl Med* 52: 769-775.  
43  
44  
45  
46 627 Locatelli E, Due RA, van den Bergh GD, van den Hoek Ostende LW. 2012. Pleistocene  
47  
48 628 survivors and Holocene extinctions: the giant rats from Liang Bua (Flores, Indonesia). *Quat Int*  
49  
50 629 19: 47-57.  
51  
52  
53  
54 630 Lokatis S, Jeschke JM. 2018. The island rule: An assessment of biases and research trends. *J*  
55  
56 631 *Biogeog* 45: 289-303.  
57

- 1  
2  
3 632 Lomolino MV. 1984. Immigrant selection, predation, and the distributions of *Microtus*  
4  
5 633 *pennsylvanicus* and *Blarina brevicauda* on islands. Am Nat 123, 468-83.  
6  
7  
8  
9 634 Lomolino MV. 1985. Body size of mammals on islands: the island rule reexamined. Am Nat  
10  
11 635 125: 310-6.  
12  
13  
14 636 Lomolino MV. 2005. Body size evolution in insular vertebrates: generality of the island rule.  
15  
16 637 J Biogeogr 32: 1683-1699.  
17  
18  
19 638 Lomolino MV, van der Geer AA, Lyras GA, Palombo MR, Sax DF, Rozzi R. 2013. Of mice  
20  
21 639 and mammoths: generality and antiquity of the island rule. J Biogeogr 40: 1427-39.  
22  
23  
24  
25 640 Louys J, Kealy S, O'Connor S, Price GJ, Hawkins S, Aplin K, Rizal Y, Zaim J, Tanudirjo DA,  
26  
27 641 Santoso WD, Hidayah AR. 2017. Differential preservation of vertebrates in Southeast Asian  
28  
29 642 caves. Int J Speleol 46: 379-408.  
30  
31  
32  
33 643 Louys J, Price GJ, O'Connor S. 2016. Direct dating of Pleistocene stegodon from Timor Island,  
34  
35 644 East Nusa Tenggara. PeerJ 10: e1788.  
36  
37  
38 645 Louys J, O'Connor S, Mahirta, Higgins P, Hawkins S, Maloney T. 2018. New genus and  
39  
40 646 species of giant rat from Alor Island, Indonesia. J Asia Pac Biodivers 11: 503-510  
41  
42  
43  
44 647 Lu D, Zhou CQ, Liao WB. 2014. Sexual size dimorphism lacking in small mammals. North-  
45  
46 648 West J Zool 10: 53–59.  
47  
48  
49 649 MacArthur RH, Wilson EO. 2016. The theory of island biogeography. Princeton, US: Princeton  
50  
51 650 University Press.  
52  
53  
54 651 Martiniaková M, Grosskopf B, Vondráková M, Omelka R, Fabiš M. 2005. Observation of the  
55  
56 652 microstructure of rat cortical bone tissue. Scripta Med 78: 45-50.

- 1  
2  
3 653 McNab BK. 1971. On the ecological significance of Bergmann's rule. *Ecol* 52: 845-854.  
4  
5  
6 654 McNab BK. 2010. Geographic and temporal correlations of mammalian size reconsidered: a  
7  
8  
9 655 resource rule. *Oecologia* 164: 13-23.  
10  
11  
12 656 McNab BK. 2019. What determines the basal rate of metabolism?. *J Exper Biol*, 222:  
13  
14 657 jeb205591.  
15  
16  
17 658 McWilliam A. 2005. Haumeni, not many: renewed plunder and mismanagement in the  
18  
19  
20 659 Timorese sandalwood industry. *Mod Asian Stud* 39: 285-320.  
21  
22  
23 660 Meiri S, Cooper N, Purvis A. 2008. The island rule: made to be broken?. *Proc R Soc Lon B*  
24  
25 661 *Biolo Sci* 275: 141-148.  
26  
27  
28 662 Meiri S, Dayan T, Simberloff D. 2004. Body size of insular carnivores: little support for the  
29  
30 663 island rule. *Am Nat* 163: 469-479.  
31  
32  
33 664 Meiri S, Dayan T, Simberloff D. 2006. The generality of the island rule reexamined. *J Biogeogr*  
34  
35 665 33: 1571-1577.  
36  
37  
38  
39 666 Michaux JR, De Bellocq JG, Sarà M, Morand S. 2002. Body size increase in insular rodent  
40  
41 667 populations: a role for predators?. *Glob Ecol Biogeog* 11: 427-436.  
42  
43  
44 668 Miller G, Spoolman S. 2011. *Living in the environment: principles, connections, and solutions.*  
45  
46 669 Belmont, US: Brooks/Cole.  
47  
48  
49  
50 670 Millien V, Damuth J. 2004. Climate change and size evolution in an island rodent species: new  
51  
52 671 perspectives on the island rule. *Evol* 58: 1353-1360.  
53  
54  
55  
56  
57  
58  
59  
60



- 1  
2  
3 672 Miskiewicz JJ. 2016. Investigating histomorphometric relationships at the human femoral  
4  
5 673 midshaft in a biomechanical context. *J Bone Miner Metab* 34: 179-192.  
6  
7  
8 674 Miskiewicz JJ, Louys J, O'Connor S. 2019. Microanatomical record of cortical bone  
9  
10 675 remodeling and high vascularity in a fossil giant rat midshaft femur. *Anat Rec* 302: 1934-1940.  
11  
12  
13  
14 676 Miskiewicz JJ, Mahoney P. 2017. Human bone and dental histology in an archaeological  
15  
16 677 context. In: Thompson T, Errickson D, eds: *Human remains: another dimension*, London, UK:  
17  
18 678 Elsevier Academic Press, 29-43.  
19  
20  
21 679 Moncunill-Solé B, Jordana X, Köhler M. 2018. Where did *Mikrotia magna* originate? Drawing  
22  
23 680 ecogeographical inferences from body mass reconstructions. *Geobios* 51: 359-366.  
24  
25  
26  
27 681 Moncunill-Solé B, Jordana X, Marin-Moratalla N, Moyà-Solà S, Köhler M. 2014. How large  
28  
29 682 are the extinct giant insular rodents? New body mass estimations from teeth and bones. *Integr*  
30  
31 683 *Zool* 9: 197-212.  
32  
33  
34  
35 684 Mullender MG, Huiskes R, Versleyen H, Buma P. 1996. Osteocyte density and  
36  
37 685 histomorphometric parameters in cancellous bone of the proximal femur in five mammalian  
38  
39 686 species. *J Orthop Res* 14: 972-979.  
40  
41  
42  
43 687 O'Connor S, Aplin K. 2007. A matter of balance: An overview of Pleistocene occupation  
44  
45 688 history and the impact of the Last Glacial Phase in East Timor and the Aru Islands, eastern  
46  
47 689 Indonesia. *Archaeol Oceania* 42: 82-90.  
48  
49  
50 690 O'Connor S, McWilliam A, Fenner JN, Brockwell S. 2012. Examining the origin of  
51  
52 691 fortifications in East Timor: social and environmental factors. *J Isl Coast Archaeol* 7: 200-218.  
53  
54  
55  
56  
57  
58  
59  
60

- 1  
2  
3 692 Orlandi-Oliveras G, Jordana X, Moncunill-Solé B, Köhler M. 2016. Bone histology of the giant  
4  
5 693 fossil dormouse *Hypnomys onicensis* (Gliridae, Rodentia) from Balearic Islands. C R Palevol  
6  
7  
8 694 15: 238-244.  
9  
10  
11 695 Oršolić N, Jeleč Ž, Nemrava J, Balta V, Gregorović G, Jeleč D. 2018. Effect of quercetin on  
12  
13 696 bone mineral status and markers of bone turnover in retinoic acid-induced osteoporosis. Pol J  
14  
15 697 Food Nutr Sci 68: 149-62.  
16  
17  
18 698 Paradis E, Schliep K. 2019. ape 5.0: an environment for modern phylogenetics and  
19  
20 699 evolutionary analyses in R. Bioinformatics 35: 526-528.  
21  
22  
23  
24 700 Palkovacs EP. 2003. Explaining adaptive shifts in body size on islands: a life history approach.  
25  
26 701 Oikos 103: 37–44  
27  
28  
29 702 Palombo MR. 2007. How can endemic proboscideans help us understand the “island rule”? A  
30  
31 703 case study of Mediterranean islands. Quat Int 169: 105-124.  
32  
33  
34  
35 704 Parra V, Jaeger JJ, Bocherens H. 1999. The skull of *Microtia*, an extinct burrowing murine  
36  
37 705 rodent of the late Neogene Gargano palaeoisland. Lethaia 32: 89-100.  
38  
39  
40 706 Paterno GB, Penone C, Werner GDA. 2018. sensiPhy: An R-package for sensitivity analysis  
41  
42 707 in phylogenetic comparative methods. Methods Ecol Evol 9: 1461-1467.  
43  
44  
45  
46 708 Pergams OR, Byrn D, Lee KL, Jackson R. 2015. Rapid morphological change in black rats  
47  
48 709 (*Rattus rattus*) after an island introduction. PeerJ 3: e812.  
49  
50  
51 710 Pianka ER. 1970. On r-and K-selection. Am Nat 104: 592-597.  
52  
53  
54  
55  
56  
57

- 1  
2  
3 711 Renaud S, Millien V. 2001. Intra-and interspecific morphological variation in the field mouse  
4  
5 712 species *Apodemus argenteus* and *A. speciosus* in the Japanese archipelago: the role of insular  
6  
7 713 isolation and biogeographic gradients. *Biol J Linn Soc* 74: 557-69.
- 8  
9  
10  
11 714 Reznick D, Bryant MJ, Bashey F. 2002. r-and K-selection revisited: the role of population  
12  
13 715 regulation in life-history evolution. *Ecol* 83: 1509-20.
- 14  
15  
16 716 Rickart EA, Heaney LR. 2002. Further studies on the chromosomes of Philippine rodents  
17  
18 717 (Muridae: Murinae). *Proc Biol Soc Wash* 115: 473-487.
- 19  
20  
21  
22 718 Russell JC, Ringler D, Trombini A, Le Corre M. 2011. The island syndrome and population  
23  
24 719 dynamics of introduced rats. *Oecologia* 167 : 667-76.
- 25  
26  
27 720 Sander PM, Mateus O, Laven T, Knötschke N. 2006. Bone histology indicates insular dwarfism  
28  
29 721 in a new Late Jurassic sauropod dinosaur. *Nature* 441: 739.
- 30  
31  
32  
33 722 Sax DF, Gaines SD. 2008. Species invasions and extinction: the future of native biodiversity  
34  
35 723 on islands. *Proc Natl Acad Sci* 105: 11490-11497.
- 36  
37  
38 724 Sengupta P. 2013. The laboratory rat: relating its age with human's. *Int J Prevent Med* 4: 624–  
39  
40 725 630.
- 41  
42  
43  
44 726 Schaub S. 1937. Ein neuer Muride von Timor. *Verhandlungen der Naturforschenden*  
45  
46 727 *Gesellschaft in Basel* 48: 1-6.
- 47  
48  
49 728 Schillaci MA, Meijaard E, Clark T. 2009. The effect of island area on body size in a primate  
50  
51 729 species from the Sunda Shelf Islands. *J Biogeogr* 36: 362-371.
- 52  
53  
54 730 Singh IJ, Gunberg DL. 1971. Quantitative histology of changes with age in rat bone cortex. *J*  
55  
56 731 *Morphol* 133: 241-51.

- 1  
2  
3 732 Sommer S, Volahy AT, Seal US. (2002). A population and habitat viability assessment for the  
4  
5 733 highly endangered giant jumping rat (*Hypogeomys antimena*), the largest extant endemic  
6  
7 734 rodent of Madagascar. *Anim Conserv* 5: 263-273.  
8  
9  
10  
11 735 Sodhi NS, Posa MR, Lee TM, Bickford D, Koh LP, Brook BW. 2010. The state and  
12  
13 736 conservation of Southeast Asian biodiversity. *Biodivers Conserv* 19: 317-28.  
14  
15  
16 737 Sondaar PY. 1977. Insularity and its effects on mammal evolution. In: Hecht MK, Goody PC,  
17  
18 738 Hecht BM, eds: *Major patterns in vertebrate evolution*, New York: Plenum Press, 671–707.  
19  
20  
21  
22 739 Stamps JA, Buechner M. 1985. The territorial defense hypothesis and the ecology of insular  
23  
24 740 vertebrates. *Quart R Biol* 60: 155-81.  
25  
26  
27 741 Swift JA, Roberts P, Boivin N, Kirch PV. 2018. Restructuring of nutrient flows in island  
28  
29 742 ecosystems following human colonization evidenced by isotopic analysis of commensal rats.  
30  
31 743 *Proc Natl Acad Sci* 115: 6392.  
32  
33  
34  
35 744 Symonds MR, Blomberg SP. 2014. A primer on phylogenetic generalised least squares. In:  
36  
37 745 Garamszegi, LZ, ed: *Modern phylogenetic comparative methods and their application in*  
38  
39 746 *evolutionary biology*, Berlin: Springer, 105-130.  
40  
41  
42  
43 747 Tate ML, Adamson JR, Tami AE, Bauer TW. 2004. The osteocyte. *Int J Biochem Cell Biol*  
44  
45 748 36: 1-8.  
46  
47  
48 749 Taylor R. 1990. Interpretation of the correlation coefficient: a basic review. *J. Diagnost. Med.*  
49  
50 750 *Sonogr* 6: 35-9.  
51  
52  
53  
54 751 Towns DR, Atkinson IA, Daugherty CH. 2006. Have the harmful effects of introduced rats on  
55  
56 752 islands been exaggerated? *Biol Invasions* 8: 863-891.  
57

- 1  
2  
3 753 van der Geer AA. 2018. Changing invaders: trends of gigantism in insular introduced rats.  
4  
5 754 Environ Conserv 45: 203-211.  
6  
7  
8 755 van der Geer AA. 2019. Effect of isolation on coat colour polymorphism of Polynesian rats in  
9  
10 756 Island Southeast Asia and the Pacific. PeerJ 7: e6894.  
11  
12  
13  
14 757 van der Geer AA, Lyras GA, Lomolino MV, Palombo MR, Sax DF. 2013. Body size evolution  
15  
16 758 of palaeo-insular mammals: temporal variations and interspecific interactions. J Biogeogr 40:  
17  
18 759 1440-1450.  
19  
20  
21 760 Van Valen LM. 1973. Patterns and the balance of nature. Evol Theor, 1: 31-49.  
22  
23  
24  
25 761 van den Hoek Ostende LW, van der Geer AA, Wijngaarden CL. 2017. Why are there no giants  
26  
27 762 at the dwarves feet? Insular micromammals in the eastern Mediterranean. Quatern Int 445: 269-  
28  
29 763 278.  
30  
31  
32 764 Ventura J, Fuster MJ. 2000. Morphometric analysis of the black rat, *Rattus rattus*, from  
33  
34 765 Congreso Island (Chafarinas Archipelago, Spain). Orsis: organismos i sistemes 15: 91-102.  
35  
36  
37  
38 766 Whittaker RJ, Fernández-Palacios JM. 2007. Island biogeography: ecology, evolution, and  
39  
40 767 conservation. Oxford: University Press.  
41  
42  
43  
44 768 Yabe T. 1994. Fat deposits for wintering in the Norway rat, *Rattus norvegicus*. J Mammal Soc  
45  
46 769 Japan 19: 129-133.  
47  
48  
49 770 Yom-Tov Y, Yom-Tov S, Moller H. 1999. Competition, coexistence, and adaptation amongst  
50  
51 771 rodent invaders to Pacific and New Zealand islands. J Biogeog 26: 947-58.  
52  
53  
54 772 Zafonte F, Masini F. 1992. Enamel structure evolution in the first lower molar of the endemic  
55  
56 773 murids of the genus *Microtia* (Pliocene, Gargano, Italy). Boll Soc Paleontol Ital 31: 335-349.  
57  
58 Miszkiewicz et al BJLS R2 Page 36 of 37  
59  
60

**FIGURE CAPTIONS**

774  
775  
776 **Figure 1.**

777  
778 The specimens examined in the present study (all caudal view) showing the size gradient in the  
779 sample and midshaft sampling location (dashed line, 1A), a histological cross-section through  
780 one of the specimens and an associated region of interest examined for osteocyte lacunae (1B),  
781 and examples of more (left) and less (right) widely dispersed osteocyte lacunae in a giant and  
782 small femora respectively (1C).

783  
784 **Figure 2.**

785  
786 Estimated body weight in grams (top), and femur midshaft measurements in medial-lateral and  
787 cranial-caudal planes in mm (bottom) for the Timor specimens (highlighted on the graph by  
788 the boxes) presented amongst other 17 known weight Asia-Pacific murine rodents.

789  
790 **Figure 3.**

791  
792 Negative allometric relationships between log estimated body mass (top row), log cranial-  
793 caudal (middle row) and log medial-lateral midshaft (bottom row) diameter data, and log  
794 osteocyte lacunae (including data corrected by midshaft size, Y axis) in the sample. Regression  
795 line is red and the confidence interval is indicated by blue lines.

796

**Table 1.** Raw data for the entire sample reporting histology and gross morphometric femoral measurements in this study: MAXL - maximum intact femur length in mm, FHDM - femoral head diameter in mm, MLW - medial-lateral midshaft femur width in mm, CCD - cranial-caudal midshaft femur depth in mm, Ot.N (a) – osteocyte lacunae number, Ot.Dn – osteocyte lacunae number (a) divided by section area (b) in mm<sup>2</sup>. \*Data from Miskiewicz et al., 2019

<b>Femur accession ID (Australian National University)</b>	<b>MAXL</b>	<b>FHDM</b>	<b>MLW</b>	<b>CCD</b>	<b>Ot.N (a)</b>	<b>Section area (b)</b>	<b>Ot.Dn (a/b)</b>
<b>TDD 1 #1</b>	n/a	n/a	7.18	5.24	2778	0.929	2990.31
<b>TDD 1 #2</b>	n/a	n/a	6.84	5.39	2380	0.927	2567.42
<b>TDD 1 #3</b>	n/a	n/a	7.25	5.89	2292	0.923	2483.21
<b>TDS 0-30 #4</b>	n/a	n/a	6.15*	4.87*	2569	0.844	3043.84
<b>TDS 15-30 #6</b>	n/a	n/a	3.59	2.31	877	0.346	2534.68
<b>TDD 1 #7</b>	n/a	n/a	4.18	3.02	1628	0.580	2806.90
<b>TDD 1 #8</b>	26.27	2.41	3.21	2.61	1218	0.375	3248.00
<b>TDD 1 #9</b>	29.73	3.51	3.85	2.5	1996	0.586	3406.14
<b>TDD 1 #10</b>	26.13	2.78	3.13	2.57	2287	0.581	3936.32
<b>TDD 1 #11</b>	n/a	n/a	2.33*	1.98*	1579	0.452	3493.36

**Table 2.** Raw data for individuals of 17 Asia-Pacific murine species of known weight and femoral midshaft size, along with the fossil specimens examined in the present study. The specimens were studied by Ken Aplin and are registered at the Commonwealth Scientific and Industrial Research Organisation (CSIRO, Australia). KMH refer to field number identifications and the two KMH specimens are deposited at Bogor Zoology Museum (Bogor, Indonesia). We use these data for illustrative purposes only (see Fig. 1). Where data were collected for more than one individual per species, the Weight, MLW, and CCD are means. Estimated body mass for the Timor fossil murines is based on a PGLS regression accounting for uncertainty in phylogenetic relationships and divergence times reported in text. \*Data from Miskiewicz et al., 2019.

Taxon/ subfamily	Comparative significance	Institution	Accession ID	Weight (g)	MLW (mm)	CCD (mm)
<i>Parahydromys asper</i>	Asian native - waterside rat of New Guinea	CSIRO	#15689	470	4.99	3.47
<i>Crossomys moncktoni</i>	Asian native - earless water rat of New Guinea	CSIRO	#15679, #15678	230 (240, 220)	3.90 (3.88, 3.92)	2.84 (2.85, 2.83)
<i>Pseudomys fumeus</i>	Southeast Australian native - smoky mouse of Australia	CSIRO	#13231	63	1.92	1.55
<i>Conilurus penicillatus</i>	Australasian native - Brush-tailed rabbit rat of Australia	CSIRO	#1007, #1009	107 (111, 103)	3.02 (2.97, 3.06)	2.77 (2.83, 2.71)
<i>Abeomelomys sevia</i>	Asian native - highland brush mouse of Papua New Guinea	CSIRO	#15693, #15694	(59.5) 64, 55	2.105 (2.33, 1.88)	1.56 (1.57, 1.54)
<i>Xeromys myoides</i>	Australasian native - false water rat of Australia and Papua New Guinea	CSIRO	#10022	44.5	2.42	1.62
<i>Hydromys habbema</i>	Asia native - mountain water rat of West Papua, Indonesia, and Papua New Guinea	CSIRO	#15691	68	2.66	1.95



<i>Mallomys istapantap</i>	Asian native - subalpine woolly rat of West Papua, Indonesia, and Papua New Guinea	CSIRO	#15681	1200	8.49	5.8
<i>Rattus fuscipes</i>	Australasian native – bush rat of Australia	CSIRO	#17928, #17927, #17922, #17201	126.75 (110, 150, 133, 114)	2.67 (2.65, 3.03, 2.71, 2.27)	2.13 (2.15, 2.28, 2.17, 1.91)
<i>Rattus lutreolus</i>	Australasian native – swamp rat of Australia	CSIRO	#6806	129	3.13	2.06
<i>Mus domesticus</i>	House mouse – included as a domesticated small rodent reference	CSIRO	#8624, #18846, #19463	14 (10, 14, 18)	1.41 (1.4, 1.33, 1.5)	1.17 (1.18, 1.18, 1.14)
<i>Paramelomys levipes</i>	Asian native - long-nosed mosaic-tailed rat or Papua New Guinea	CSIRO	#15695	44	1.64	1.46
<i>Pogonomys loriae</i>	Asian native - tree mouse of Australia, Indonesia, and Papua New Guinea.	CSIRO	#16516	62	2.19	1.95
<i>Protochromys fellowsi</i>	Asian native - red-bellied mosaic-tailed rat of Papua New Guinea	CSIRO	#16504	98	2.73	1.85
<i>Melomys burtoni</i>	Australasian native - grassland mosaic-tailed rat of Australia and Papua New Guinea	CSIRO	#3673	40	1.79	1.74
<i>Mammelomys sp.</i>	Asian native - rodent genus endemic to New Guinea	KMH	#1893	116	2.72	2.6
<i>Rattus praetor</i>	Asian native - large spiny rat of Papua New Guinea, and the Solomon Islands	KMH	#1833	435	4.81	3.49
Murinae spp.	Asian material used in this study	ANU	TDD 1 #1	1015	7.18	5.24
Murinae spp.		ANU	TDD 1 #2	990	6.84	5.39
Murinae spp.		ANU	TDD 1 #3	1188	7.25	5.89
Murinae spp.		ANU	TDS 0-30 #4	765	6.15*	4.87*
Murinae spp.		ANU	TDS 15-30 #6	156	3.59	2.31
Murinae spp.		ANU	TDD 1 #7	262	4.18	3.02
Murinae spp.						

Murinae spp.		ANU	TDD 1 #8	158	3.21	2.61
Murinae spp.		ANU	TDD 1 #9	187	3.85	2.5
Murinae spp.		ANU	TDD 1 #10	150	3.13	2.57
Murinae spp.		ANU	TDD 1 #11	75	2.33*	1.98*

For Peer Review

**Table 3.** Data for the entire murine sample representing femoral morphometric and histological measurements: N – sample size, MIN. = minimum value of data, MAX. – maximum value of data, SD – standard deviation.

VARIABLES	N	MIN.	MAX.	MEAN	SD
MAXL	3	26.13	29.73	27.38	2.04
FHDM	3	2.41	3.51	2.90	0.56
MLW	10	2.33	7.25	4.77	1.88
CCD	10	1.98	5.89	3.64	1.51
Ot.N (#)	10	877.00	2778.00	1960.40	615.87
Section area (mm <sup>2</sup> )	10	0.35	0.93	0.65	0.23
Ot.Dn (#/mm <sup>2</sup> )	10	2483.21	3936.32	3051.02	474.99
Ot.Dn/ MLW	10	342.51	1499.30	766.03	393.57
Ot.Dn/ CCD	10	421.60	1764.32	1002.32	472.12

**Table 4.** Spearman's *Rho* correlations and ordinary least squares (OLS) regressions assessing relationships between osteocyte lacunae and rat femur size and estimated body mass (using raw and log transformed data respectively): coefficient of determination ( $r^2$ ), slope ( $b$ ), confidence interval (CI), intercept ( $Y$ ), Total sample size is 10 in each test. \*statistically significant at  $p < 0.05$ ; †statistically significant at Bonferroni corrected  $p < 0.017$ .

<b>X axis</b>	<b>Y axis</b>	<b>Rho</b>	<b>p</b>
estimated body mass (g)	Ot.Dn (#/mm <sup>2</sup> )	-0.661	<0.038*
	Ot.Dn/CCD	-0.939	<0.0001*†
	Ot.Dn/MLW	-0.952	<0.0001*†
CCD (mm)	Ot.Dn (#/mm <sup>2</sup> )	-0.576	0.082
	Ot.Dn/CCD	-0.915	<0.0001*†
	Ot.Dn/MLW	-0.891	0.001*†
MLW (mm)	Ot.Dn (#/mm <sup>2</sup> )	-0.721	0.019*
	Ot.Dn/CCD	-0.952	<0.0001*†
	Ot.Dn/MLW	-0.976	<0.0001*†
<b>OLS X axis</b>	<b>Y axis</b>	<b><math>r^2</math>, <math>b</math>, <math>Y</math>, <math>CI</math></b>	<b>p</b>
log estimated body mass	log Ot.Dn	0.367, -0.092, 8.546, -0.178 -0.024	0.064
	log Ot.Dn/CCD	0.952, -0.498, 9.678, -0.568 -0.429	<0.0001*†
	log Ot.Dn/MLW	0.917, -0.491, 9.361, -0.560 -0.418	<0.0001*†
log CCD	log Ot.Dn	0.317, -0.210, 8.268, -0.415 -0.028	0.090
	log Ot.Dn/CCD	0.940, -1.211, 8.269, -1.436 -1.036	<0.0001*†
	log Ot.Dn/MLW	0.864, -1.167, 7.94, -1.486 -0.920	<0.0001*†
log MLW	log Ot.Dn	0.409, -0.243, 8.376, -0.436 -0.069	0.046*
	log Ot.Dn/CCD	0.937, -1.233, 8.637, -1.432 -0.965	<0.0001*†
	log Ot.Dn/MLW	0.947, -1.244, 8.378, -1.432 -1.058	<0.0001*†

1  
2  
3  
4  
5  
6  
7  
8  
9  
10  
11  
12  
13  
14  
15  
16  
17  
18  
19  
20  
21  
22  
23  
24  
25  
26  
27  
28  
29  
30  
31  
32  
33  
34  
35  
36  
37  
38  
39  
40  
41  
42  
43  
44  
45  
46

For Peer Review

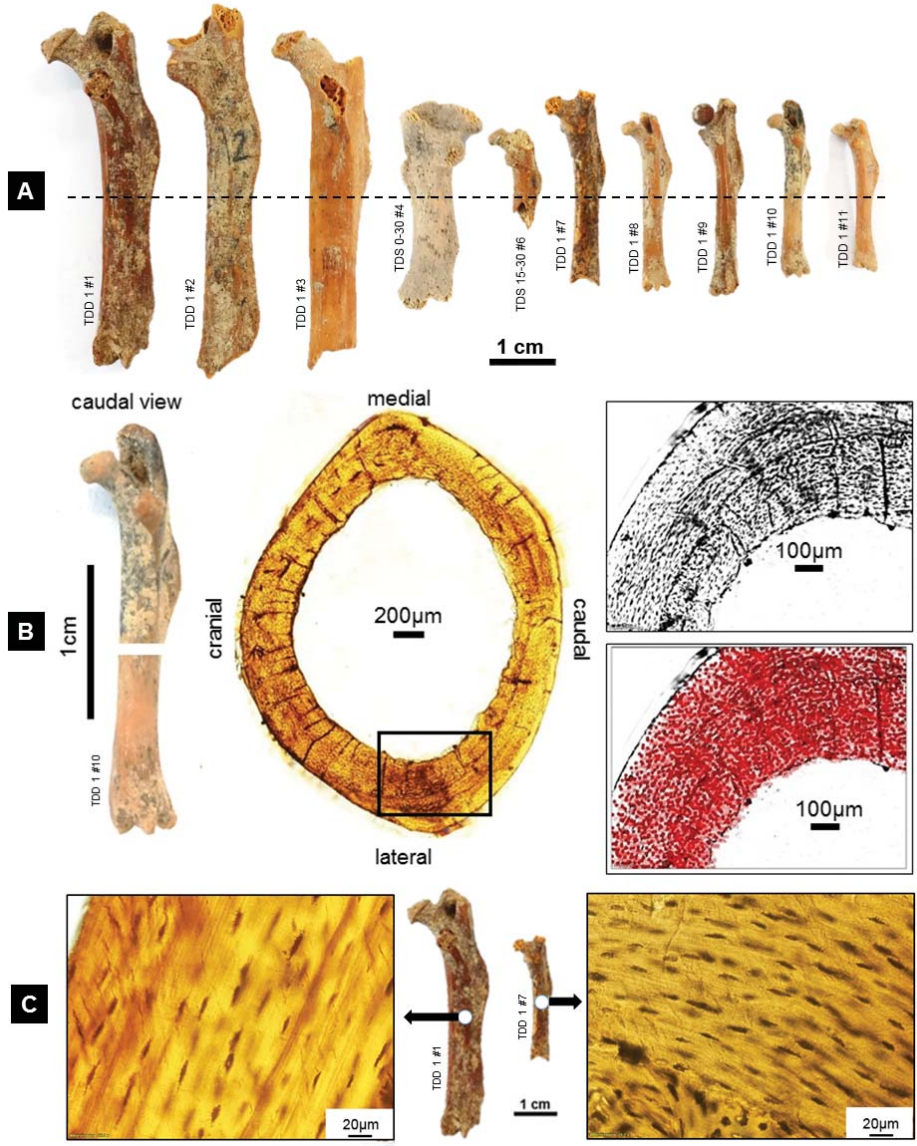


Figure 1.

The specimens examined in the present study (all caudal view) showing the size gradient in the sample and midshaft sampling location (dashed line, 1A), a histological cross-section through one of the specimens and an associated region of interest examined for osteocyte lacunae (1B), and examples of more (left) and less (right) widely dispersed osteocyte lacunae in a giant and small femora respectively (1C).

250x310mm (96 x 96 DPI)

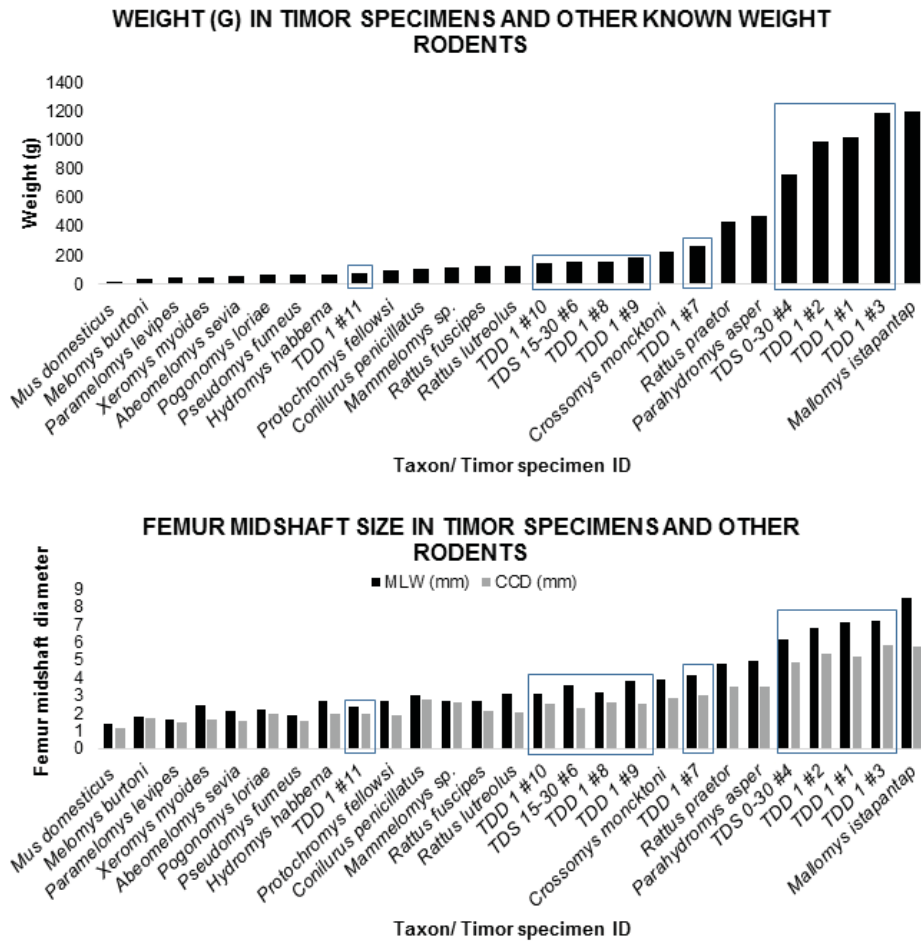


Figure 2.

Estimated body weight in grams (top), and femur midshaft measurements in medial-lateral and cranial-caudal planes in mm (bottom) for the Timor specimens (highlighted on the graph by the boxes) presented amongst other 17 known weight Asia-Pacific murine rodents.

179x175mm (96 x 96 DPI)

1  
2  
3  
4  
5  
6  
7  
8  
9  
10  
11  
12  
13  
14  
15  
16  
17  
18  
19  
20  
21  
22  
23  
24  
25  
26  
27  
28  
29  
30  
31  
32  
33  
34  
35  
36  
37  
38  
39  
40  
41  
42  
43  
44  
45  
46  
47  
48  
49  
50  
51  
52  
53  
54  
55  
56  
57  
58  
59  
60

**BODY WEIGHT, FEMUR SIZE, AND OSTEOCYTE LACUNAE RELATIONSHIPS**

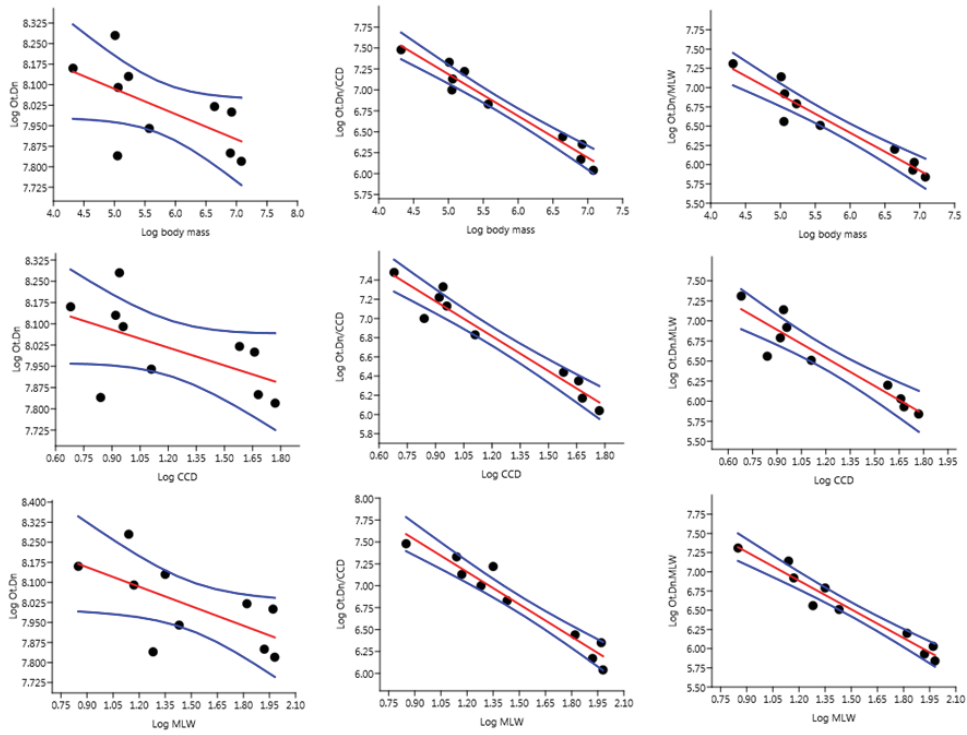


Figure 3.

Negative allometric relationships between log estimated body mass (top row), log cranial-caudal (middle row) and log medial-lateral midshaft (bottom row) diameter data, and log osteocyte lacunae (including data corrected by midshaft size, Y axis) in the sample. Regression line is red and the confidence interval is indicated by blue lines.

236x187mm (96 x 96 DPI)